2084 *Macromolecules* **2010**, *43*, 2084–2087
DOI: 10.1021/ma902571h

Macromolecules
NOTE

High Pressure Phase Diagram of an Aqueous PEO-PPO-PEO Triblock Copolymer System via Probe Diffusion Measurements

Christopher J. Kloxin and John H. van Zanten*

Department of Chemical and Biomolecular Engineering, North Carolina State University, Raleigh, North Carolina 27695-7905

Received November 22, 2009; Revised Manuscript Received January 15, 2010

ABSTRACT: Phase diagrams of soft fragile materials are typically determined via static structural methods, such as small angle neutron scattering (SANS; Mortensen, K.; Pedersen, J. S. *Macromolecules* **1993**, *26* (4), 805−812), small-angle X-ray scattering (Lodge, T. P.; Pudil, B.; Hanley, K. J. *Macromolecules* **2002**, *35* (12), 4707−4717), or light scattering (Brown, W.; Schillen, K.; Almgren, M.; Hvidt, S.; Bahadur, P. *J. Phys. Chem.* **1991**, *95* (4), 1850−1858). Dynamical methods, such as rheometry, can also be employed since the relaxation spectrum varies greatly from one phase to another. Unfortunately, mechanically disturbing these systems can alter the underlying fragile structures, precluding quiescent state determination. Here, a method for determining soft matter phase diagrams utilizing high-frequency tracer microrheology measurements is demonstrated for an aqueous PEO-PPO-PEO triblock copolymer system over a full range of temperatures and hydrostatic pressures. Since the tracer particle thermal motion reflects the underlying suspending media dynamics, the delicate fluid structure is preserved. Readily discernible changes in the tracer particle thermal motion are observed to be associated with morphological phase transitions, and the determined phase boundaries compare favorably with SANS data found in the literature.

I. Introduction

Tracer microrheological measurements of complex materials have garnered much attention owing to their ability to capture a material's linear viscoelastic behavior without perturbing the underlying structure.[1] Recent theoretical developments have provided a framework to interpret the motion of embedded tracers as the response to the suspending material's viscoelastic susceptibility.[1] Subsequently, several complex materials, such as polymer solutions,[1−4] associating polymer solutions,[5−8] and worm-like micelles (WLM),[9−12] have been examined utilizing diffusing wave spectroscopy (DWS)[13,14] of a dilute particle suspension at frequencies inaccessible to traditional rheological methods (∼O (1 MHz)).

While static scattering methods provide invaluable structural information in the Fourier domain, dynamic scattering methods yield structural evolution information. Previous workers have demonstrated the use of high pressure DWS to explore the aggregation behavior of sterically stabilized silica spheres.[15] Here, we extend this work by demonstrating that DWS measurements are well suited for rapidly characterizing morphological phase transitions in complex fluids at high pressure. Specifically, the microrheology of an aqueous triblock copolymer solution is measured over a full range of temperatures and hydrostatic pressures exceeding 200 MPa, utilizing a high pressure transmission scattering cell originally designed for SANS experiments.[16,17] Aqueous Pluronic solutions are known to exhibit a rich phase behavior as a function of both temperature and pressure.[18−21] As the material undergoes a morphological phase transition, there is a distinct change in tracer particle mean square displacement temporal behavior, thereby providing a facile method for *rapidly* constructing high pressure phase diagrams for complex fluids.

*Corresponding author. E-mail: john_vz@ncsu.edu.

II. Results and Discussion

Aqueous Pluronic solutions are PEO-PPO-PEO (poly(ethylene oxide)-*b*-poly(propylene oxide)-*b*-poly(ethylene oxide)) triblock copolymers that generally exhibit lower critical solution temperature (LCST) behavior, where the central PPO block has a lower LCST than the peripheral PEO blocks. Under ambient conditions, 25 wt % P85 in D_2O exists as micelles, with a PPO core surrounded by a PEO corona.[18] In contrast with typical monodispersed diblock copolymers, there is a temperature range over which individual Pluronic chains (i.e., unimers) within the micelle are in dynamic exchange with the surrounding solution.[22,23] As the temperature is elevated, more unimers become incorporated into the micelle fraction, whereas increasing hydrostatic pressure increases the solvent quality, driving the unimers from the micelle to the surrounding media.

In Figure 1, the P85 in D_2O solution exhibits an initial shift to higher microscopic creep values with raised hydrostatic pressure, which subsequently decreases gradually upon further hydrostatic pressure elevation. This distinct shift in the creep compliance is characteristic of an interacting to noninteracting micellar transition. As the creep compliance scales t^1, the underlying micellar solution structure does not display a mechanism for energy storage on the micellar time scales (those time scales shown here).[24] To better illustrate this phenomenon, the viscosity is extracted from the microscopic creep data (see Supporting Information) and shown in Figure 2. The viscosity of a micellar solution, η, can be expressed as the product of the underlying solvent viscosity and a function of the micelle volume fraction as $\eta = \eta_s f(\phi)$, where η_s increases with unimer bulk concentration and $f(\phi)$ increases with increasing volume fraction.[25] The transfer of Pluronic molecules from micelles to the bulk solution with increasing pressure results in a decrease in micelle volume fraction and an increase in the underlying solvent viscosity. In the dilute regime, the interplay between micelle volume fraction and solvent

 Published on Web 01/28/2010

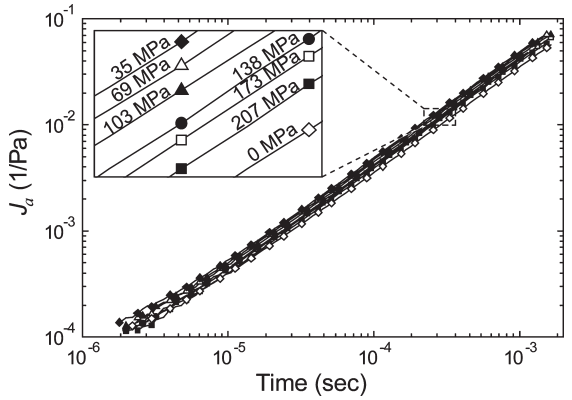

Figure 1. Microscopic creep vs time for a sample of 25 wt % P85 in D_2O at 20 °C measured for increasing hydrostatic pressure from 0 to 207 MPa. The microscopic creep traces are parallel but demonstrate a nonmonotonic response with the initial increase in hydrostatic pressure [from 0 MPa (open diamond) to 35 MPa (closed diamond)].

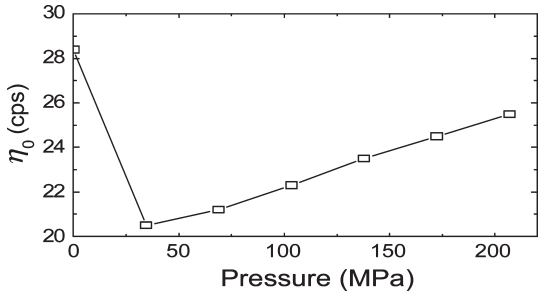

Figure 2. Zero-frequency viscosity vs hydrostatic pressure found by fitting the long-time data given in Figure 1 (25 wt % P85 in D_2O at 20 °C).

viscosity is described by the Einstein equation for the viscosity of a suspension of dilute, noninteracting spheres, $\eta = \eta_s(1 + 2.5\phi)$, which excludes two-body interactions. The high pressure, linear regime shown in Figure 2 suggests the dynamics are not dominated by the micelle volume fraction of the solution but rather the contribution of the unimer enriched solution surrounding the micelles. That is, the "solvent" viscosity rises faster than $f(\phi)$ decreases. Nevertheless, this dilute solution description does not account for the ambient pressure shift to higher viscosity, and nondilute, higher-order interactions must be considered. Thus, the initial viscosity decrease is attributed to the system undergoing an interacting to noninteracting or semidilute to dilute micellar transition: an effect also observed by Cabana et al.[26] Alternatively, the ambient pressure micelles may exhibit a 'sticky' or attractive interaction potential.[24]

In comparison with the 20 °C isotherm, higher temperature isotherms exhibit significantly different dynamical fingerprints. In Figure 3a and b (the 35 and 45 °C isotherms, respectively), there is a transition from a viscous liquid ($J_a(t) \sim t^{\alpha}$, $\alpha \cong 1$) to a viscoelastic liquid ($J_a(t) \sim t^{\alpha}$, $\alpha < 1$) upon decreasing pressure. Prior to micellar crystal formation, a coexistence of crystalline and isotropic regions is predicted to occur.[27] The two microscopic creep traces at the lowest pressures in Figure 3a and b are indicative of this coexistence. Further decreasing the pressure yields a flat region whose relaxation occurs beyond the time-scales considered here (note that the ambient pressure is not displayed in either panel).

Although both the 35 and 45 °C isotherms exhibit similar trends upon approach to the micellar crystalline region, the high-pressure behavior indicates a slightly different character for each temperature. At the highest pressures, the 35 °C isotherm begins

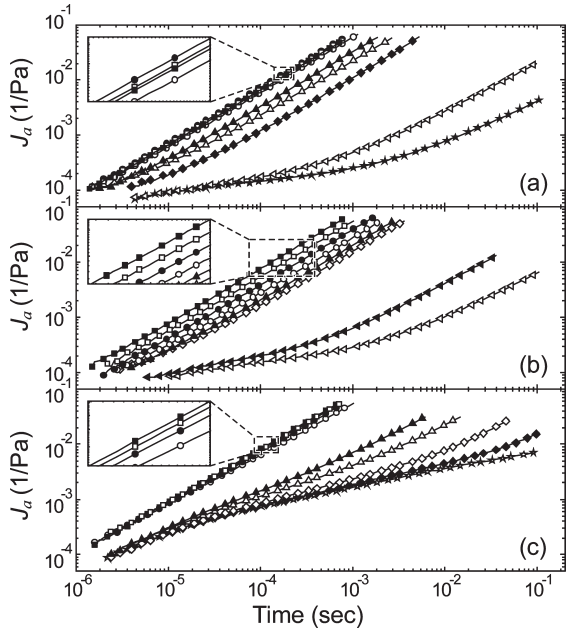

Figure 3. Microscopic creep compliance of 25 wt % P85 in D_2O as a function of hydrostatic pressure for the (a) 35, (b) 45, and (c) 70 °C isotherms. The symbols indicate 207 (■), 172 (□), 138 (●), 103 (○), 68.9 (▲), 51.7 (△), 34.5 (◇), 17.2 (◆), 12.4 (left-pointing solid triangle), 10.3 (left-pointing open triangle), 9.7 (★), 0 MPa (☆). The insets show expanded regions of the plot, highlighting trends in the high pressure data.

to show a noninteracting-to-interacting micellar transition previously recognized at the 20 °C isotherm. Over the same pressure range, the 45 °C isotherm is still within the interacting micellar regime as indicated by the strong pressure dependence of the microscopic creep and therefore the viscosity. This trend of solvent quality increasing with increasing pressure and decreasing temperature is similar to that observed in other aqueous Pluronic systems.[20]

Ambient pressure SANS studies, reported by Mortensen et al.,[18,28,29] indicate a transition from a disordered to a cubic micellar paracystralline phase occurs at intermediate temperatures in a 25 wt % aqueous P85 solution. Increasing temperature revealed a transition into another disordered micelle phase followed by micellar growth into elongated or rod-like micelles. The dynamical behavior of these two phases is apparent in the 35, 45, and 70 °C tracer particle thermal motion data shown in Figure 3. Furthermore, the 70 °C tracer particle mean square displacement temporal variation shown in Figure 3c has a significantly different sol-to-gel transition than observed for the 35 and 45 °C isotherms. First, the sol-to-gel transition occurs over a much larger range of pressure, from 69 MPa to ambient. This is consistent with the picture of micellar growth leading to longer terminal-relaxation times. Second, the developing creep plateau modulus is at least an order of magnitude larger for the high temperature gel compared to the low temperature solid. Moreover, it appears that the developing creep plateau modulus is less flat (i.e., larger slope) for the higher temperature gel. Finally, there is a distinct transition between high and low pressures at high frequencies (i.e., short-times).

The two high frequency limiting behaviors observed in the 70 °C microscopic creep data reflects the underlying micellar hydrodynamics of the system. At high pressure, the microscopic creep data is reminiscent of a micellar cluster forming Pluronic system (L64).[24] However, rather than phase separating upon decreasing solvent quality, the aqueous P85 system undergoes a transition into an elongated or worm-like micellar (WLM) phase. At low pressure, the micellar high-frequency limiting behavior

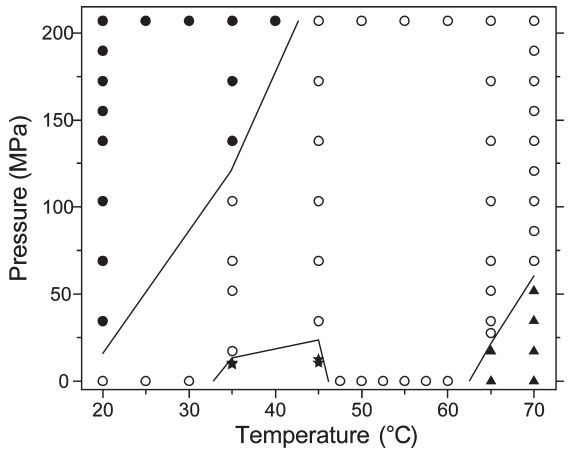

Figure 4. T−P phase diagram for 25 wt % P85 in D_2O as determined by DWS microrheology. Circles represent liquid-like micellar phase where closed and open circles represent noninteracting and interacting micelles, respectively; stars and triangles represent solid-like BCC and cylindrical phases, respectively. The lines are drawn as an approximate boundary between areas of differing behavior.

most likely reflects the micellar hydrodynamics at length-scales smaller than entanglement. A similar phenomenon is observed in DWS measurements of a cetyl pyridinium chloride/sodium salycilate WLM system.[30] This observation further highlights the potential of DWS microrheology to probe high-frequency dynamics in such thermally sensitive systems, where time−temperature superposition is not applicable.

With the collection of microscopic creep traces over a vast range of temperature and pressure phase-space, one can construct a phase diagram based on dynamical properties. To obtain a three-dimensional representation, each microscopic creep must be reduced to a single parameter representing the same "dynamical" characteristic of each curve. Here, the pressure where the microscopic creep exhibits temporal scaling $J(t) \sim t^{\alpha}$, with $\alpha \leq 1/2$, will denote the formation of a solid-like material, even if short-lived. Such a designation is consistent with solid-like to liquid-like transitions as defined within the framework of linear viscoelasticity. As seen in the microscopic creep traces, further decreasing pressure results in the solids becoming longer lived. Although this analysis is restricted to a temporal range determined by the experimental configuration, the investigated time-scale is most sensitive to a transition from Pluronic micelles to larger length-scale structures because it encompasses the single micelle self-diffusion time.[24]

The phase diagram, shown in Figure 4, was generated using a survey of 60 data sets, and indicates the presence of two solid-like regions: (*i*) a low temperature solid corresponding to micellar crystalline structure and (*ii*) a high temperature gel corresponding to entangled rod-like (or worm-like) micelles. Application of hydrostatic pressure to either solid-like phase effectively melts each one, yielding a liquid-like sol. Although high pressure structural data was not found in the literature for the current system, pressure melting has been observed in other aqueous Pluronic systems (e.g., an aqueous F88 Pluronic solution).[22] The phase envelopes identified at ambient pressure are slightly reduced in comparison with ambient SANS measurements;[18,19,28] however, this most likely owes to the adopted 1/2 power scaling criterion to discriminate between solid-like and liquid-like phases. Temporal scaling of less than one indicates energy storage and, hence, the presence of appreciable fluid structure. By using a scaling criterion of < 1, a similar phase envelope correspondence between DWS and SANS measurements is achieved. Finally, a transition from noninteracting to interacting micelles is recognized, exemplifying the potential of DWS measurements to characterize the dynamical behavior of such systems.

III. Concluding Remarks

The influence of hydrostatic pressure on the dynamical properties of a 25 wt % P85 in D_2O solution as reflected by the thermal motion of embedded probe particles is shown to be a suitable method for rapidly determining complex fluid phase diagrams. The disorder-to-order transition is marked by a shift from a microscopic creep temporal scaling of one to less than one (i.e., diffusive to subdiffusive probe particle mean square displacement scaling). These experimental observations indicate the presence of two distinctly different solid-like regions in phase-space, as observed in ambient pressure SANS measurements.[18,19,28] It is not surprising, given the inherent relationship between structure and dynamics, that DWS tracer studies provide a corresponding viewpoint of the phase behavior of the system. However, DWS tracer studies allow unique access to high frequency quiescent sol−gel transitions in soft fragile matter, which may allow more detailed causal analysis directly linking structure to property.

Acknowledgment. This work was supported by the National Science Foundation under Grant Nos. CTS-00960219 (originally CTS-9702413) and CTS-9700170. C.J.K. and J.v.Z. are also thankful for further support from Kodak.

Supporting Information Available: Experimental details regarding the sample preparation, high pressure DWS, and data interpretation. This material is available free of charge via the Internet at http://pubs.acs.org.

References and Notes

(1) Mason, T. G.; Weitz, D. A. *Phys. Rev. Lett.* **1995**, *74* (7), 1250–1253.
(2) van Zanten, J. H.; Amin, S.; Abdala, A. A. *Macromolecules* **2004**, *37* (10), 3874–3880.
(3) Papagiannopoulos, A.; Fernyhough, C. M.; Waigh, T. A. *J. Chem. Phys.* **2005**, *123* (21), 214904.
(4) Dasgupta, B. R.; Tee, S. Y.; Crocker, J. C.; Frisken, B. J.; Weitz, D. A. *Phys. Rev. E* **2002**, *65* (5), 051505.
(5) Lu, Q.; Solomon, M. J. *Phys. Rev. E* **2002**, *66* (6), 061504.
(6) Sprakel, J.; van der Gucht, J.; Stuart, M. A. C.; Besseling, N. A. M. *Phys. Rev. E* **2008**, *77* (6), 061502.
(7) Knoben, W.; Besseling, N. A. M.; Bouteiller, L.; Stuart, A. C. *Phys. Chem. Chem. Phys.* **2005**, *7* (11), 2390–2398.
(8) van der Gucht, J.; Besseling, N. A. M.; Knoben, W.; Bouteiller, L.; Stuart, M. A. C. *Phys. Rev. E* **2003**, *67* (5), 051106.
(9) van Zanten, J. H.; Rufener, K. P. *Phys. Rev. E* **2000**, *62* (4), 5389–5396.
(10) Cardinaux, F.; Cipelletti, L.; Scheffold, F.; Schurtenberger, P. *Europhys. Lett.* **2002**, *57* (5), 738–744.
(11) Raudsepp, A.; Callaghan, P.; Hemar, Y. *J. Rheol.* **2008**, *52* (5), 1113–1129.
(12) Bellour, M.; Skouri, M.; Munch, J. P.; Hebraud, P. *Eur. Phys. J. E* **2002**, *8* (4), 431–436.
(13) Pine, D. J.; Weitz, D. A.; Chaikin, P. M.; Herbolzheimer, E. *Phys. Rev. Lett.* **1988**, *60* (12), 1134–1137.
(14) Weitz, D. A.; Pine, D. J. *Diffusing-Wave Spectroscopy*; Oxford University Press: Oxford, 1993; p 735.
(15) Vavrin, R.; Kohlbrecher, J.; Wilk, A.; Ratajczyk, M.; Lettinga, M. P.; Buitenhuis, J.; Meier, G. *J. Chem. Phys.* **2009**, *130* (15), 13.
(16) Kermis, T. W.; Li, D.; Guney-Altay, O.; Park, I. H.; van Zanten, J. H.; McHugh, M. A. *Macromolecules* **2004**, *37* (24), 9123–9131.
(17) Lesemann, M.; Nathan, H.; DiNoia, T. P.; Kirby, C. F.; McHugh, M. A.; van Zanten, J. H.; Paulaitis, M. E. *Ind. Eng. Chem. Res.* **2003**, *42* (25), 6425–6430.
(18) Mortensen, K.; Pedersen, J. S. *Macromolecules* **1993**, *26* (4), 805–812.
(19) Mortensen, K. *Europhys. Lett.* **1992**, *19* (7), 599–604.
(20) Mortensen, K.; Schwahn, D.; Janssen, S. *Phys. Rev. Lett.* **1993**, *71* (11), 1728–1731.
(21) Kostko, A. F.; Harden, J. L.; McHugh, M. A. *Macromolecules* **2009**, *42* (14), 5328–5338.
(22) Cau, F.; Lacelle, S. *Macromolecules* **1996**, *29* (1), 170–178.

(23) Hvidt, S.; Trandum, C.; Batsberg, W. *J. Colloid Interface Sci.* **2002**, *250* (1), 243–250.
(24) Kloxin, C. J.; van Zanten, J. H. *J. Chem. Phys.* **2009**, *131* (13), 10.
(25) Larson, R. G. *The Structure and Rheology of Complex Fluids*; Oxford University Press: New York, 1999.
(26) Cabana, A.; AitKadi, A.; Juhasz, J. *J. Colloid Interface Sci.* **1997**, *190* (2), 307–312.
(27) Hoover, W. G.; Ree, F. H. *J. Chem. Phys.* **1968**, *49* (8), 3609–3617.
(28) Mortensen, K. *J. Phys.: Condes. Matter* **1996**, *8* (25A), A103–A124.
(29) Mortensen, K. *Polym. Adv. Technol.* **2001**, *12* (1−2), 2–22.
(30) Oelschlaeger, C.; Schopferer, A.; Scheffold, F.; Willenbacher, N. *Langmuir* **2009**, *25* (2), 716–723.